

Correlation between Hemichrome Stability and the Root Effect in Tetrameric Hemoglobins

Alessandro Vergara,^{†‡} Marisa Franzese,[†] Antonello Merlino,^{†‡} Giovanna Bonomi,[†] Cinzia Verde,[§] Daniela Giordano,[§] Guido di Prisco,[§] H. Caroline Lee,[¶] Jack Peisach,[¶] and Lelio Mazzeola^{†‡*}

[†]Department of Chemistry, University of Naples “Federico II”, Complesso Universitario Monte S. Angelo, Naples, Italy; [‡]Istituto di Biostrutture e Bioimmagini, and [§]Institute of Protein Biochemistry, Consiglio Nazionale delle Ricerche, Naples, Italy; and [¶]Department of Physiology and Biophysics, Albert Einstein College of Medicine, Yeshiva University, New York, New York

ABSTRACT Oxidation of Hbs leads to the formation of different forms of Fe(III) that are relevant to a range of biochemical and physiological functions. Here we report a combined EPR/x-ray crystallography study performed at acidic pH on six ferric tetrameric Hbs. Five of the Hbs were isolated from the high-Antarctic notothenioid fishes *Trematomus bernacchii*, *Trematomus newnesi*, and *Gymnodraco acuticeps*, and one was isolated from the sub-Antarctic notothenioid *Cottoperca gobio*. Our EPR analysis reveals that 1), in all of these Hbs, at acidic pH the aquomet form and two hemichromes coexist; and 2), only in the three Hbs that exhibit the Root effect is a significant amount of the pentacoordinate (5C) high-spin Fe(III) form found. The crystal structure at acidic pH of the ferric form of the Root-effect Hb from *T. bernacchii* is also reported at 1.7 Å resolution. This structure reveals a 5C state of the heme iron for both the α - and β -chains within a T quaternary structure. Altogether, the spectroscopic and crystallographic results indicate that the Root effect and hemichrome stability at acidic pH are correlated in tetrameric Hbs. Furthermore, Antarctic fish Hbs exhibit higher peroxidase activity than mammalian and temperate fish Hbs, suggesting that a partial hemichrome state in tetrameric Hbs, unlike in monomeric Hbs, does not remove the need for protection from peroxide attack, in contrast to previous results from monomeric Hbs.

INTRODUCTION

Hbs are proteins that are devoted to oxygen transport in blood. They carry out their function when the iron atom, which binds the oxygen molecule, is in the reduced Fe(II) state. However, it is well known that Hbs may undergo spontaneous oxidation even under physiological conditions. Although the ferric forms are physiologically inert to further oxygenation, several subsequent side reactions in the Hb autoxidation may interfere with or merge into other biochemical pathways. Oxidized Hbs are involved in a range of biomedical and physiological functions. For example, autoxidation is a serious problem because it limits the storage time of acellular Hb-based blood substitutes (1). In addition to the commonly observed aquomet and hydroxylmet species, oxidation of Hbs can lead to the formation of pentacoordinate and endogenous hexacoordinate species, including bis-His adducts (hemichromes) (2).

In the past, hemichromes were considered to be precursors of Hb denaturation because their formation is accelerated by denaturing agents (3). More recently, it was shown that hemichromes can be obtained under nondenaturing as well as physiological conditions (4). However, the physiological role of hemichromes is still disputed. It has been suggested that bis-His adducts can be involved in nitric oxide (NO) detoxification by acting as a NO scavenger (5), in the *in vivo* reduction of met-Hb, in Heinz-body formation (3), and in ligand binding (6,7). Hemichrome detection may also represent a valuable tool for tumor diagnosis (8). More recently, hemichromes were suggested to be involved in protecting Hbs from peroxide attack (9), given that the hemichrome derivative of human α -subunit complexed with AHSP does not exhibit peroxidase activity.

Under physiological conditions, mammalian Hbs contain a low level of hemichrome. In contrast, Antarctic fish Hbs at room temperature are easily oxidized to a partial hemichrome state in which only the iron of the β -chain is bonded to the distal histidine (10–13). Cold adaptation (e.g., the biosynthesis of antifreeze glycoproteins) and isolation due to the Antarctic polar front are the major peculiarities of the Antarctic Notothenioidei (the dominant suborder of teleosts in the Southern ocean), but other features, such as the high mitochondrial content of slow muscle fibers (14), can also be cold-adaptive. Despite the high level of sequence homology among the different members, Antarctic fish Hbs show marked differences in their functional properties, and therefore provide an intriguing system in which to explore the structural determinants and functional role of

Submitted November 24, 2008, and accepted for publication April 28, 2009.

*Correspondence: lelio.mazzeola@unina.it

Abbreviations used: Hbs, hemoglobins; AHSP, α -hemoglobin stabilizing protein; bis-His, bis-histidyl; CT, charge transfer; CW-EPR, continuous-wave electron paramagnetic resonance; deo-HbTb, the deoxy form of HbTb at pH 6.0; Hb, hemoglobin; HbA, adult human hemoglobin; Hb1Cg, Hb1 of *Cottoperca gobio*; HbGa, Hb of *Gymnodraco acuticeps*; Hb1Tn, major Hb of *Trematomus newnesi*; Hb2Tn, minor Hb of *Trematomus newnesi*; HbCTn, cathodic Hb of *Trematomus newnesi*; HbTb, Hb of *Trematomus bernacchii*; hemi-HbTb, the β -bis-histidyl ferric form of HbTb at pH 7.6; pH6-HbTb, the ferric form of HbTb at pH 6.0; PDB, Protein Data Bank; TrI, Hb I of trout; RMSD, root mean-square deviation; TrIV, Hb IV of trout; T state, tense state.

Editor: Marilyn Gunner.

© 2009 by the Biophysical Society
0006-3495/09/08/0866/9 \$2.00

doi: 10.1016/j.bpj.2009.04.056

hemichrome formation (15). Crystallographic studies of the major Hbs from the Antarctic fish *Trematomus bernacchii* and *Trematomus newnesi* at pH 7.6 have revealed that the hemichrome derivative at physiological pH is associated with a quaternary assembly that is intermediate between the R and T states (10,11). In this form (hereafter denoted the H state), several features of the tertiary organization are also intermediate.

In addition to hemichrome formation, some Antarctic fish Hbs also display a drastic reduction of the oxygen affinity and binding rate coupled with a loss of cooperativity at the lower values of the physiological pH range (16,17). This property, known as the Root effect (17), is also common to several Hbs of temperate fish. Many unsuccessful attempts to interpret the Root effect on structural grounds have been conducted in the past and include sequence comparison (18), site-directed mutagenesis (19), and x-ray structural comparison of Root-effect and non-Root-effect Hbs. Based on crystallographic analysis, the most current hypothesis attributes the Root effect to overstabilization of the T quaternary structure at physiological pH (20,21), although tertiary-structure features may modulate the strength of the effect (21,22).

We recently characterized the oxidized states of five Hbs isolated from the Antarctic fish species *T. bernacchii* (HbTb), *T. newnesi* (Hb1Tn, Hb2Tn, and HbCTn), and *Gymnodraco acuticeps* (HbGa) by EPR at physiological pH (11). That investigation revealed the existence of a variety of ferric forms, ranging from aquomet/hydroxymet to two distinct hemichromes, including the presence of a pentacoordinate (5C) high-spin Fe(III) form. Of interest, some Hbs of Arctic fish can also adopt a 5C high-spin Fe(III) form, and in solution show only a low content of hemichrome species (11,23).

In the investigation presented here, we explored the interconnection between hemichrome stability and Root-effect occurrence by using a combined EPR/x-ray crystallography method to study the oxidation of six notothenioid Hbs at acidic pH. Our data reveal that the two hemichromes observed at physiological pH (11) persist at acidic pH in the five Hbs from the Antarctic species *T. bernacchii*, *T. newnesi*, *G. acuticeps*, as well as in the Hb of the sub-Antarctic species *Cottoperca gobio* (Hb1Cg). The choice of these six Hbs was motivated by the fact that, although in the ferric state they form the α (aquomet)/ β (bis-His) derivative, only three of them exhibit the Root effect (HbTb, HbCTn, and Hb1Cg), whereas the remaining three (HbGa, Hb1Tn, and Hb2Tn) are scarcely sensitive to pH. The results indicate that the three Hbs endowed with the Root effect have a larger amount of the 5C Fe(III) form at acidic pH in comparison with the other three. Moreover, x-ray analysis of ferric HbTb crystallized at pH 6.0 shows that the latter is in the 5C-coordination state and adopts a T quaternary structure. The observation that the 5C forms are present in Antarctic fish Hbs in a suite of pH conditions prompted us to investigate whether these proteins are endowed with a peroxidase

function. Indeed, all of these Antarctic fish Hbs (both with and without the Root effect) exhibit a much higher peroxidase activity than human and temperate fish Hbs, suggesting that a partial hemichrome state in tetrameric Hbs does not remove the need for protection from peroxide action, in contrast to previous results from monomeric Hbs (9).

MATERIALS AND METHODS

Hb purification

Purification and storage of HbTb (24); Hb1Tn, Hb2Tn, and HbCTn (25); HbGa (26); and the major Hb from *C. gobio* (Hb1Cg) (27) were performed as previously described. Hbs were oxidized with $K_3Fe(CN)_6$, and the excess was removed by gel filtration on a Sephadex G-25 column.

EPR

Ferric Hbs were studied by means of CW-EPR at 12 K using a Bruker ESP 300 spectrometer equipped with an Oxford Instrument ESR 10 continuous-flow cryostat and model 3120 temperature controller. Data were exported to Bruker WinEPR, version 2.11, for processing in a manner similar to that previously described (11,23). All EPR samples were at 0.5 mM tetramer concentration. The buffers (50 mM citrate pH 4.5, MES pH 6.0, HEPES pH 7.6, and BICINE pH 9.0 and 10.4) were chosen for their low protonation enthalpy (28). Spectra were recorded at 9.29-GHz microwave frequency, 10-mW microwave power, 100-kHz modulation frequency, and 5-G modulation amplitude.

Optical spectroscopy

Optical pH titration of HbTb was performed in a JASCO 530V spectrophotometer. The buffers were the same as those used for the EPR analysis.

X-ray crystallography

In a first attempt, crystals grown at pH 7.6 (11) were equilibrated in a step-wise fashion in mother liquor with a final pH value of 6.0. In all trials, the crystals readily developed cracks on their surface and became disordered. Direct crystallization of oxidized HbTb (pH6-HbTb) was performed in a capillary at pH 6.0 and room temperature by means of the liquid-diffusion technique (final conditions 6.0 mg/mL HbTb and 8% w/v MPEG 5K), which provided well-diffracting crystals.

Diffraction data on pH6-HbTb were collected at high resolution (1.7 Å) with the XRD1 beam line of the Elettra Synchrotron (Trieste, Italy). A data set was collected at 100 K using glycerol as the cryoprotectant and processed with the program suite HKL (29). A summary of the data-processing statistics is provided in Table 1. Crystals of pH6-HbTb were isomorphous to those of deoxy HbTb (21,30). A statistical analysis of the intensities indicates that the diffraction data are affected by pseudo-merohedral twinning similar to that previously described in detail for deoxy HbTb crystals (30). The twin fraction for the crystal used in the data collection is 0.47, as determined by the algorithm implemented in the program SHELX (31). Despite twinning, the high resolution of the diffraction pattern still allows a highly significant refinement of the model. The coordinates of the high-resolution (1.3 Å) deoxy structure of HbTb (PDB code 2H8F) (21) were used as a starting model, which was then refined using the program SHELX-L (31). The refinement runs were followed by manual intervention using the molecular graphic program O (32) to correct minor errors in side-chain positions. Water molecules were identified by evaluating the shape of the electron density and the distance of potential hydrogen-bond donors and/or acceptors. At convergence, the R-factor value was 0.156 ($R_{free} = 0.204$). A summary of the refinement statistics is given in Table 1. The coordinates of the structure have been deposited in the PDB with entry code 3GQG.

TABLE 1 Data collection and refinement statistics

Diffraction data	
Space group	P2 ₁
Cell parameters	
a (Å)	61.72
b (Å)	94.78
c (Å)	61.72
β (°)	90.09
Resolution range (Å)	30.00–1.71 (1.76–1.71)*
No. of unique reflections	69821
Completeness (%)	95.1 (88.1)*
R _{merge} (%)	4.3 (17.5)*
I/σ(I)	31.6 (5.1)
Redundancy	3.7
Refinement	
Resolution range (Å)	30.00–1.71
R (%)	15.0
R _{free} (%)	20.8
No. of protein atoms	4449
No. of water molecules	405
RMSD	
Bond lengths (Å)	0.010
Bond angles (°)	2.28
Average atomic displacement	
Main chain (Å ²)	20.8
Side chain (Å ²)	22.7
Whole chain (Å ²)	21.7
Heme (Å ²)	23.3
Water molecules (Å ²)	27.5

*Numbers in parentheses refer to the outermost shell.

Heme geometry

To compare the heme coordination of pH6-HbTb with those of other hemoproteins, we performed a statistical analysis of the structure of the heme regions in all of the globin structures in the PDB. In particular, we found 998 iron-containing hemes in 317 crystal structures of Hbs, myoglobins, or leghemoglobins. All data analyses were performed using programs developed in-house.

Peroxidase assays

Peroxidase activity was measured in HbTb, HbGa, and *T. newnesi* hemolysate at 20°C according to a published procedure (33), using dopamine and guaiacol as substrates. The data are the average of three independent kinetic traces. The peroxidase activity of HbA was measured as a control to reproduce the literature data (34). In the cases of HbTb and HbA, the experiments were also repeated at 4°C at the highest Hb concentration used for the 20°C data.

RESULTS

EPR and optical spectra

The EPR spectra of the six ferric Hbs from *T. bernacchi* (HbTb), *T. newnesi* (Hb1Tn, Hb2Tn, and HbCTn), *G. acuticeps* (HbGa), and *C. gobio* (Hb1Cg) at pH 6.0 show both an axial high-spin ferric signal and two rhombic low-spin ferric signals (Fig. 1). High-spin signals with identical *g*-values (5.88 and 2.01) were found in HbTb, Hb1Tn, Hb2Tn, HbCTn, Hb1Cg, and HbGa, but the *g* = 5.88 signal of HbTb, Hb1Cg, and HbCTn (Fig. 1, left panel) exhibited an increase in rhombicity (11) compared with that of the other

Hbs (Fig. 1, inset). Two sets of low-spin signals with *g*_{max} and *g*_{mid} values of 3.2 and 2.3/2.2, 2.9, and 2.3/2.2, 2.6, and 2.2, respectively, were resolved for the six Hbs (Fig. 1, right panel). In addition, a third low-spin signal was detected in HbCTn (2.6 and 2.2).

The *g*-values for the two low-spin signals fall into class B of the Truth Table (35), which comprises bis-His and bis-imidazole complexes. These data are indicative of the presence of two distinct hemichromes, as observed at physiological pH in Antarctic fish Hbs (11) and Hb1Cg (see Fig. S1 in the Supporting Material). These findings reveal that the two hemichromes are partially persistent and stable at moderately acidic pH. In agreement with our previous findings (11), hemichrome II (*g* = 2.9, 2.3/2.2) has a less anisotropic EPR signal, has *g*-values close to those of cytochrome *b*₅, and is less abundant than hemichrome I (*g* = 3.2, 2.3/2.2) in HbTb, Hb1Tn, Hb2Tn, HbGa, and Hb1Cg. However, in HbCTn, hemichrome II is more abundant than hemichrome I (Fig. 1, right panel).

The third low-spin form of HbCTn (*g* = 2.6, 2.2) arises from a hydroxymet form (class O of the Truth Table published by Peisach (35)). This indicates that in HbCTn hydroxymet is persistent at pH 6.0, and suggests that the pK_a of the ferric heme-bound water molecule is lower than in the other five Hbs.

The dominant high-spin signal in the six Hbs (*g* = 5.88, 2.01) corresponds to that of an aquomet form. The rhombic distortion of this high-spin signal in HbTb, HbCTn, and Hb1Cg (Fig. 1, left panel, inset) suggests the formation of unligated, pentacoordinated Fe (III). Such forms were previously observed in EPR and crystallographic studies of distal histidine mutants of myoglobin (36,37), in peroxidases (38), in a flavo Hb (39), in a giant Hb at acidic pH (40), and in *Scapharca inequivalvis* Hb (41). Although we note that buffer-dependent rhombic distortion of the high-spin signal of the hexacoordinate aquomet form has been observed (36), x-ray crystal structures and EPR studies of HbTb performed here and in a previous work (11) strongly suggest that the rhombic high-spin signals found in Antarctic fish Hbs are due to pentacoordinate ferric hemes. HbCTn also partially shows this form at physiological pH (11).

A more extended analysis of the pH dependence of the distribution of the ferric species was also conducted on Root-effect HbTb. The EPR data of HbTb at different pH values (4.5, 6.0, 9.0, and 10.4) are reported in Fig. 2 together with data previously obtained at pH 7.6 (11). 5C forms appear at high and low pH (Fig. 2, inset; the signal intensities were normalized against those at pH 7.6 to underline the increase in rhombicity at low and high pH). The 5C form (*g* = 6.1) is dominant at pH 4.5. As judged by comparing EPR spectra at different pHs, formation of the 5C form appears to be associated with a decrease of the hemichrome content (see pH 6.0 and 4.5). As expected, the hydroxymet content (*g* = 2.6, 2.2) increases with pH. The reversibility of the form was checked by optical spectroscopy, and it

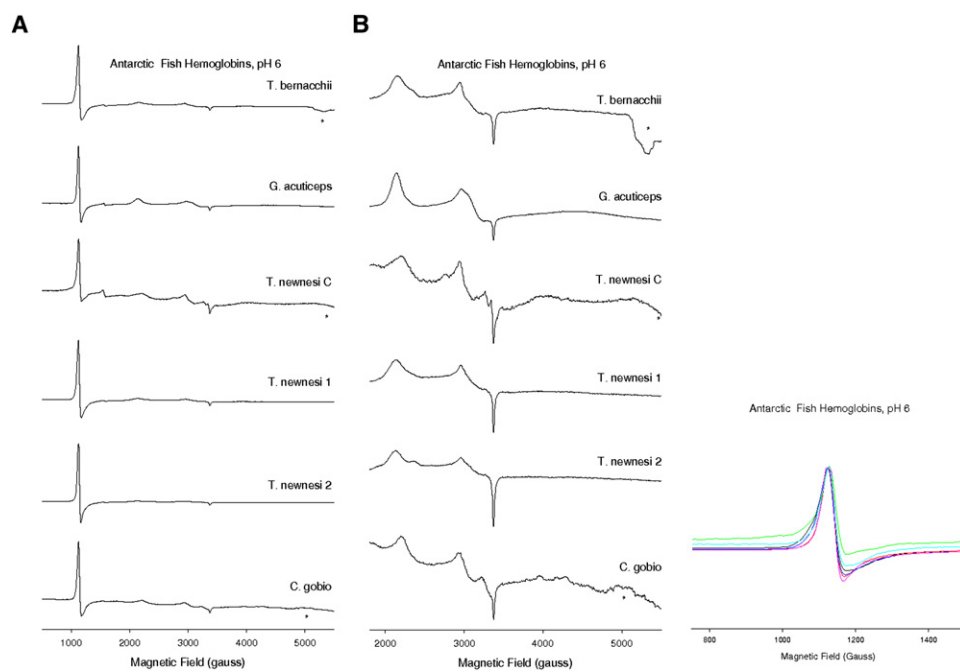


FIGURE 1 CW-EPR spectra of six notothenioid ferric Hbs: HbTb, HbGa, HbCTn, Hb1Tn, Hb2Tn, and Hb1Cg. The protein concentration was 0.5 mM tetramer, and the buffer was 50 mM HEPES pH 6.0. Spectra were recorded at 12 K, microwave frequency of 9.29 GHz, microwave power of 10 mW, modulation frequency of 100 kHz, and modulation amplitude of 5 G. Spectra in the left panel are replotted on a $\times 10$ intensity scale on the right, showing the low-spin signal region. (Baseline artifacts are present in the high-field region of some of the spectra and are marked by asterisks.) The $g = 5.88$ regions of the high-spin signals are shown in the inset: *T. bernacchii* (HbTb, Root effect; black), *G. acuticeps* (HbGa, no Root effect; red), *T. newnesi* C (HbCTn, Root effect; green), *T. newnesi* 1 (Hb1Tn, no Root effect; blue), *T. newnesi* 2 (Hb2Tn, no Root effect; pink), and *C. gobio* (Hb1Cg, Root effect; cyan). The signal intensities are normalized against that of HbTb. The increase in line width in the down-field region of the signal indicates an increase in rhombicity.

was found that irreversible protein unfolding took place only at $\text{pH} > 9.0$. It is likely that under denaturing conditions, low-spin hexacoordinated forms, possibly coming from endogenous non-His residues, can be formed.

The optical spectra of HbTb as a function of pH (from pH 4.5 to 9.0) are reported in Fig. S2. As shown by these spectra, the CT band at 630 nm, corresponding to the high-spin axial ferric species (aquomet), does not follow a monotonic trend. The CT band goes up from pH 9.0 to pH 6.0 (due

to the conversion of the hydroxymet to the aquomet species (12)), but below 6.0 it slightly decreases with the decrease in concentration of the bis-histidyl adduct (as judged by the intensities of the bands at 530 and 565 nm), together with the concomitant appearance of a band at 652 nm.

Crystal structure of oxidized HbTb at pH 6.0

To characterize the pH dependence of iron coordination in ferric Antarctic fish Hbs on a structural basis, we elucidated

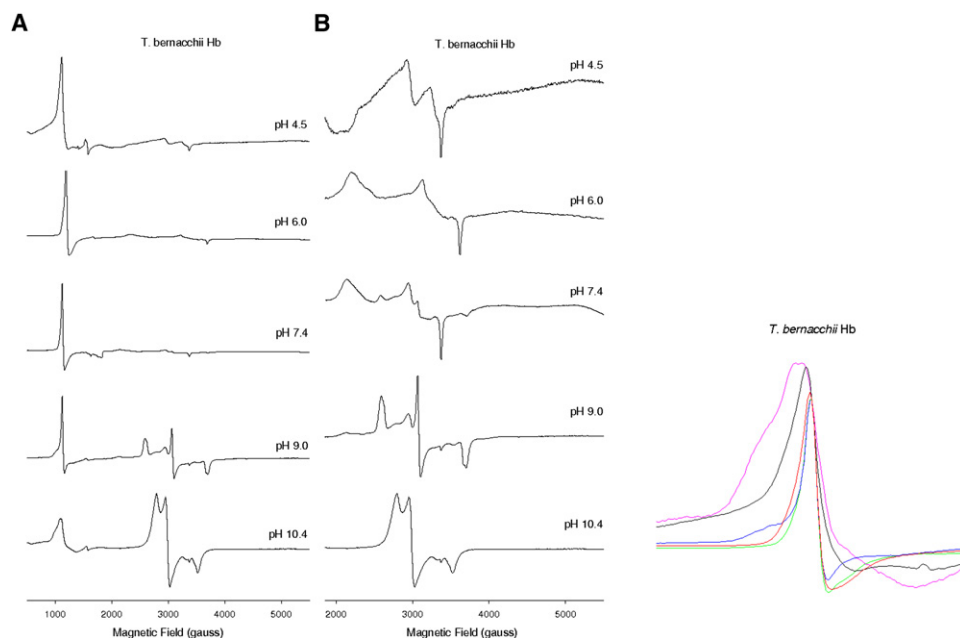


FIGURE 2 CW-EPR spectra of ferric HbTb at different pH values. Experimental conditions as in Fig. 1. Spectra in the left panel are replotted on a $\times 10$ intensity scale on the right, showing the low-spin signal region. The $g = 5.88$ regions of the high-spin signals are shown in the inset: pH 4.5 (black), pH 6.0 (red), pH 7.6 (green), pH 9.0 (blue), and pH 10.0 (pink). The signal intensities are normalized against that of the pH 7.6 sample. The increase in line width in the down-field region of the signal indicates an increase in rhombicity.

the novel structure of the oxidized form of HbTb at pH 6.0 (pH6-HbTb) using synchrotron data at 1.7 Å resolution (Table 1) and compared it with that solved at pH 7.6 (11). Although crystals are affected by pseudo-merohedral twinning, the resolution of the diffraction pattern ensures sufficient data to produce a well-refined molecular structure, as evidenced by the good quality of the omit electron density maps for most of the residues (Figs. 3–5), the distribution of the thermal displacement parameters (Table 1), and the final refinement statistics (crystallographic R-factor = 0.156, $R_{\text{free}} = 0.204$) The RMSD of the C^α atoms between the two halves $\alpha_1\beta_1$ and $\alpha_2\beta_2$ of the tetramer, related by a noncrystallographic twofold axis, is only 0.26 Å.

The crystallographic model demonstrates that at acidic pH the iron-to-histidine bond on the distal side of the hemi-HbTb (PDB code 2PEG) β -chain (11) is broken, and the molecule modifies the quaternary structure to adopt the typical quaternary T structure of the deoxy ferrous state. Indeed, the RMSD between the C^α atoms of pH6-HbTb and deo-HbTb (PDB code 2H8F) (21) is only 0.19 Å, which has to be compared with the value of 1.39 Å for the superposition of the structure presented here with that obtained at pH 7.6. With respect to the latter, the stacking interaction between the imidazole groups of the two C-terminal histidines observed at the $\beta_1\beta_2$ interface at physiological pH is broken (Fig. 5 B). The β C-terminus moves away from the molecular diad to a position very close to that occupied in the classical T structure, with Tyr-145 placed in the tyrosine pocket interacting with the FG corner (residues 94–98) (Fig. 4) and the terminal carboxyl group hydrogen-bonded to the amino group of Lys-40 α . The full attainment of the T structure is completed with the exclusion of the water molecule that in hemi-HbTb mediates the contact between the carboxyl groups of Asp-95 α and Asp-101 β at the $\alpha_1\beta_2$ ($\alpha_2\beta_1$) interface, and the formation of a strong hydrogen bond between the two aspartates (Fig. 5 A). The similarity of this structure with that of deo-HbTb also extends to the formation of the salt bridges between His-55 and Asp-48 in the α -chains and His-72 and Asp-69 in the β -chains, which are considered

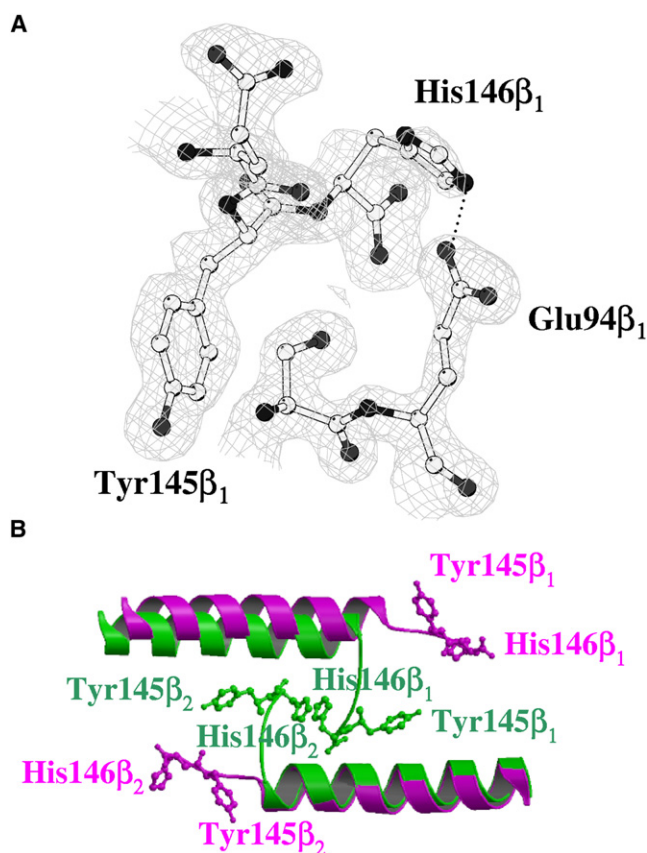


FIGURE 4 (A) Omit Fo-Fc electron density maps contoured at 3.0σ at the β C-terminus of one chain of pH6-HbTb. (B) $\beta_1\beta_2$ interfaces of HbTb observed in T (purple) and H (green) quaternary structure, after superposition of one chain. The alternative conformation of the His-146 side chain is removed for clarity.

relevant for the Root effect (21,22). Moreover, the β -iron(III) is pentacoordinated, in similarity to the mixed oxidized form of Hb1 from *T. newnesi* at pH 7.6 refined at a resolution of

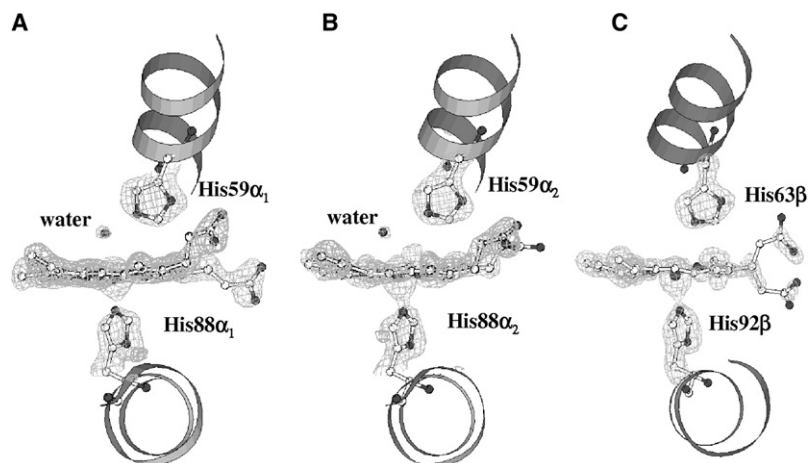


FIGURE 3 Omit Fo-Fc electron density maps contoured at 3.0σ of pH6-HbTb: (A) α_1 -heme, (B) α_2 -heme, and (C) β -heme.

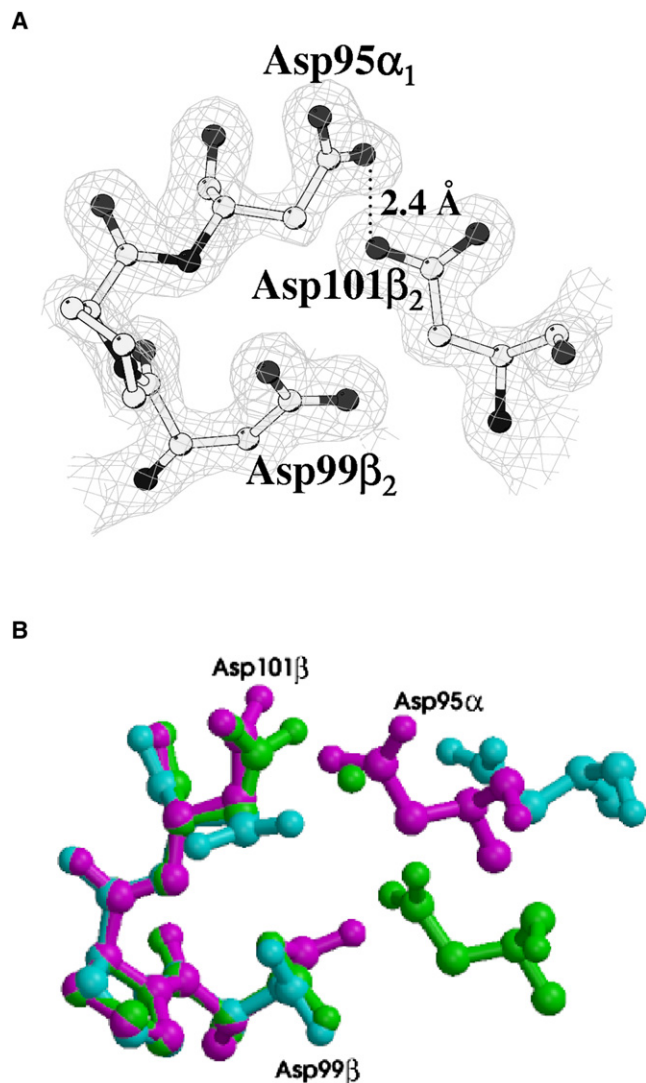


FIGURE 5 (A) Omit $F_o - F_c$ electron density map contoured at 3.0σ at the $\alpha_1\beta_2$ interface of pH6-HbTb. (B) Superimposed $\alpha_1\beta_2$ interfaces of HbTb observed in the T (purple), R (cyan), and H (green) quaternary structures.

1.25 Å, which is characterized by distinct binding and oxidation states of the α - and β -chains (13).

The main differences between the structure of this oxidized form of HbTb and the reduced one at pH 6.0 are observed at the α -heme pockets (Fig. S3), where densities interpreted as water molecules are found in the map of the pH6-HbTb crystal. In one chain, the neatly shaped density is centered at 2.3 Å from the iron ion and the water molecule refines with a rather low thermal displacement parameter ($B = 23.7 \text{ \AA}^2$). Also, the His-59 side chain swings out slightly with respect to the deo-HbTb form to make more room for the water molecule, which is hydrogen-bonded to the $N^{\epsilon 2}$ of His at 2.8 Å (Fig. S3 A). In the second chain, the density is more diffuse and centered at 2.97 Å from the metal. A survey of about 1000 heme geometries from the x-ray structure of Hbs, myoglobins in their met-form depos-

ited in the PDB, gives an average iron-to-water distance of $2.08 \pm 0.04 \text{ \AA}$ and indicates that the value for this distance observed in the first chain might still be considered in the longer side of the distribution tail. However, since for the second chain the distance is far too large for the water molecule to be considered as an iron ligand, we shall consider the α -chains to be in the 5C state. A large variability of the distal water position with respect to the heme iron(III) has also been noted in various cytochromes (42).

Taking advantage of the strict isomorphism between the deo-HbTb and pH6-HbTb crystals, we independently validated the densities in the distal pockets by calculating a difference Fourier map with the coefficient $(|F_d| - |F_p|) \exp(i\varphi_d)$, where $|F_d|$ and $|F_p|$ are the observed structure amplitudes of deo-HbTb and pH6-HbTb, respectively, and φ_d are the phases of deo-HbTb. This map does not rely on the phases of the modeled pH6-HbTb structure; instead, it relies only on its observed structure amplitudes. The densities from this isomorphous difference map are very similar to those reported in Fig. 3. Other subtle differences between the structures of ferric and ferrous HbTb at pH 6 are observed at His-45 α (Fig. S3 B), which is more ordered in pH6-HbTb than in deo-HbTb. In the former, His-45 α is salt-bridged to the propionate group of the heme and is hydrogen-bonded to a water molecule that in turn is linked to the side chain of Ser-44 α (Fig. S3 B).

The authors are aware of the possibility that the intense x-ray synchrotron radiation may reduce the metal center, as has been observed, for instance, in peroxide-derived myoglobin intermediates (43); however, this phenomenon does not seem to be relevant in this case, for the following reasons: First, when we attempted to prepare the reduced iron(II) form of the hemichrome (the so-called hemochrome species) by reducing crystals of HbTb76 grown at pH 7.6 with dithionite, the crystals were severely damaged (44). This observation indicates that the hemochrome form is not stable and is spontaneously converted into the isomeric T deoxy state, in line with the spectroscopic data obtained from solution at the same pH. Crystal damage was also observed when the pH of the crystallization mixture, containing crystals of hemi-HbTb at pH 7.6, was progressively reduced to pH = 6.0 under oxidizing conditions, thus indicating some modification of the quaternary structure at acidic pH not connected to the reduction of the iron center. Third, crystals of the form presented here were also preliminarily tested on an in-house diffractometer and proved to be isomorphous with that used in the data collection experiment. Finally, electron density maps showed no trace of disordering effects, which are expected to show up when some modification of the molecular structure is progressively brought about during exposure to the x-ray beam. Thus, on the basis of the combined spectroscopic and crystallographic data on pH6-HbTb, we believe that if any reduction had occurred under exposure to the x-ray beam of the synchrotron, it must have occurred within a molecular structure that already

possessed all of the relevant features discussed above. Some minor local effects, such as that observed at the distal site of one of the α -chains, could instead be explained by progressive reduction of the iron ion.

Peroxidase activity

The peroxidase activity was investigated in HbTb, HbGa, and *T. newnesi* hemolysates at 20°C, with dopamine used as the substrate. The data are plotted in Fig. 6 as a function of Hb concentration, together with literature data on HbA (as a control of reproducibility) and other temperate fish Hbs (34). A significant increase in peroxidase activity can be observed in all Antarctic fish Hbs with respect to the other Hbs reported in Fig. 6, and this activity follows a Michaelis-Menten behavior. Similar results were obtained with HbTb using guaiacol as the substrate. Measurements were also repeated on HbA and HbTb at 4°C, and the results show that the peroxidase activity is not significantly affected by temperature, at least in the range of 4–20°C.

DISCUSSION

The H quaternary structure of ferric HbTb at physiological pH is modified when the pH decreases. Indeed, the crystal structure of the 5C form of ferric HbTb at pH 6.0 (pH6-HbTb) reveals a T quaternary structure. These data suggest that the strong T-state stabilization at acidic pH, related to the Root effect in ferrous Hbs, also persists in the ferric state of HbTb. This constraint is so strong as to make ferrous deo-HbTb (21) very similar to ferric pH6-HbTb. The crystallo-

graphic model of pH6-HbTb also provides a structural explanation of the pH-modulated quaternary transition in the ferric state of HbTb. In particular, the change at the $\alpha_1\beta_2$ interface, together with the breakage of the salt bridges His-72 β -Asp-69 β and His-55 α -Asp-48 α , reveals the source of protons released upon the T \rightarrow H transition, and thus the pH dependence of this allosteric equilibrium (21,22). It should be recalled that this quaternary-structure transition is associated with a drastic change in the coordination of the heme iron from unligated $\alpha(5C)/\beta(5C)$ to ligated $\alpha(\text{aquo})/\beta(\text{bis-His})$.

EPR spectra collected from five Antarctic fish Hbs and a sub-Antarctic species (Hb1Cg) reveal that the ferric forms at neutral pH (aquomet and two distinct hemichromes) persist at acidic pH. However, only in the three Root-effect Hbs is a pentacoordinate (5C) high-spin Fe(III) form, which according to the pH6-HbTb structure comes from a decrease in hemichrome population, also observed. The pH titration of HbTb followed by EPR and optical spectroscopy from pH 10.4 to 4.5 supports the crystallographic analysis. Indeed, the data obtained at pH 4.5 suggest a strong decrease of the low-spin 6C form in favor of a high-spin 5C state.

Altogether, the crystallographic/EPR evidence of pH-induced hemichrome \rightarrow 5C conversion in Root-effect Hbs and the crystallographic evidence of a pH-induced quaternary H \rightarrow T transition in ferric HbTb suggest that hemichrome is not compatible with the T quaternary structure. Therefore, the Root effect, via over-stabilization of the T state at acidic pH, may also function in the ferric state by modulating the hemichrome stability. This putative incompatibility between hemichrome and the T state may arise from the difficulty of bending helices E and F enough to reduce the C $^{\alpha}$ -C $^{\alpha}$ distance between proximal and distal His from 14.0–14.5 Å to 12.0–12.5 Å to allow endogenous coordination (13).

A 5C ferric state has also been observed at physiological pH as a product of autoxidation (11,13) and in polar Hbs with Val \rightarrow Ile67 β -replacement (11,23). But what are the consequences of the accessibility of reactive 5C ferric states in Antarctic fish Hbs? The presence of a 5C form, which is typical of hemoproteins with redox properties, under a variety of pH conditions suggests an additional functional role of ferric Hb in Antarctic fish. As in other tetrameric Hbs (33), Antarctic fish Hbs exhibit peroxidase activity. According to the current hypothesis regarding hemichrome's role in protecting Hbs from peroxide attack (9), the activity of Antarctic fish Hbs of *T. newnesi*, *T. bernacchi*, and *G. acuticeps*, which can form stable hemichromes, should be less than half that of aquomet HbA. In contrast, the measured peroxidase activity of Antarctic fish Hbs is much higher (by 10-fold) than that of mammalian Hbs, and even higher than that of temperate fishes (34) (Fig. 6). The enhanced peroxidase activity of Antarctic fish Hbs compared with temperate fish Hbs suggests that the presence of a bis-His complex at the β -heme does not protect against peroxide attack. These data are not necessarily in disagreement with

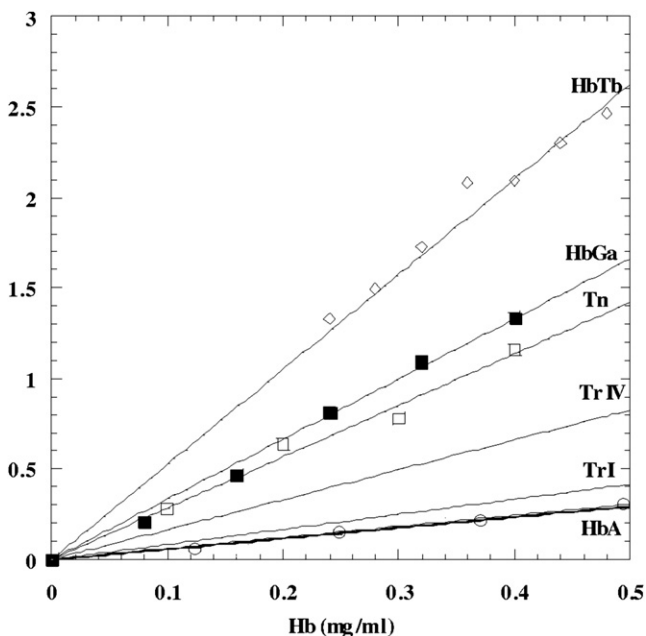


FIGURE 6 Peroxidase activity of HbTb, HbGa, and the hemolysate of *T. newnesi* (Tn). Literature data for Hb I and IV of trout (TrI and TrIV) and HbA are also reported.

previous reports on the α -chain of ferric HbA complexed with AHSP (9) and ferric myoglobin in the presence of linoleic acid (45,46). The tetrameric nature of Antarctic fish Hbs and the communication between α - and β -hemes may justify the different behavior of these partial hemichrome states (4).

According to the evidence of high peroxidase activity at physiological temperature, the exchange between hemichrome and 5C forms may play a distinctive physiological role in Antarctic teleosts, and it could compensate for the lower Hb concentration often found in Antarctic fishes, in addition to protecting against higher oxidative stress related to the high mitochondrial content of slow muscle fibers.

SUPPORTING MATERIAL

Three figures are available at [http://www.biophysj.org/biophysj/supplemental/S0006-3495\(09\)00981-3](http://www.biophysj.org/biophysj/supplemental/S0006-3495(09)00981-3).

We thank the Elettra Synchrotron (Trieste, Italy) for providing time on the beam line, and the staff of the beam line XRD1 for assistance during data collection. We also thank Giosuè Sorrentino and Maurizio Amendola for their technical assistance.

This work was supported financially by the Italian National Programme for Antarctic Research, within the framework of the Evolution and Biodiversity in the Antarctic program sponsored by the Scientific Committee for Antarctic Research, and by the Ministero Italiano dell'Università e della Ricerca Scientifica (PRIN 2007 "Struttura, funzione ed evoluzione di emoproteine da organismi marini artici ed antartici: meccanismi di adattamento al freddo e acquisizione di nuove funzioni"). A.V. received travel grants from the University of Naples and the Albert Einstein College of Medicine. Work carried out at the Albert Einstein College of Medicine was supported by the National Institutes of Health (grants GM040168 and HL071064-03004 to J.P.).

REFERENCES

- Ray, A., B. A. Friedman, and J. M. Friedman. 2002. Trehalose glass-facilitated thermal reduction of metmyoglobin and methemoglobin. *J. Am. Chem. Soc.* 124:7270–7271.
- Rachmilewitz, E. A., J. Peisach, and W. E. Blumberg. 1971. Stability of oxyhemoglobin A and its constituent chains and their derivatives. *J. Biol. Chem.* 246:3356–3366.
- Rifkind, J. M., O. Abugo, A. Levy, and J. Heim. 1994. Detection, formation, and relevance of hemichromes and hemochromes. *Methods Enzymol.* 231:449–480.
- Vergara, A., L. Vitagliano, G. di Prisco, C. Verde, and L. Mazzarella. 2008. Spectroscopic and crystallographic characterization of hemichromes in tetrameric hemoglobins. *Methods Enzymol.* 436A:421–440.
- Smaghe, B., J. T. I. Trent, and M. S. Hargrove. 2008. NO dioxygenase activity in hemoglobins is ubiquitous in vitro, but limited in vivo. *PLoS ONE.* 3:1–10.
- de Sanctis, D., A. Pesce, M. Nardini, M. Bolognesi, A. Bocedi, et al. 2004. Structure-function relationships in the growing hexa-coordinate hemoglobin sub-family. *IUBMB Life.* 56:643–651.
- Pesce, A., D. De Sanctis, M. Nardini, S. Dewilde, L. Moens, et al. 2004. Reversible hexa- to penta-coordination of the heme Fe atom modulates ligand binding properties of neuroglobin and cytoglobin. *IUBMB Life.* 56:657–664.
- Croci, S., G. Pedrazzi, G. Passeri, P. Piccolo, and I. Ortalli. 2001. Acetylphenylhydrazine induced haemoglobin oxidation in erythrocytes studied by Mossbauer spectroscopy. *Biochim. Biophys. Acta.* 1568: 99–104.
- Feng, L., S. Zhou, L. Gu, D. Gell, J. Mackay, et al. 2005. Structure of oxidized α -haemoglobin bound to AHSP reveals a protective mechanism for haem. *Nature.* 435:697–701.
- Riccio, A., L. Vitagliano, G. di Prisco, A. Zagari, and L. Mazzarella. 2002. The crystal structure of a tetrameric hemoglobin in a partial hemichrome state. *Proc. Natl. Acad. Sci. USA.* 99:9801–9806.
- Vergara, A., M. Franzese, A. Merlino, L. Vitagliano, G. di Prisco, et al. 2007. Structural characterization of ferric hemoglobins from three Antarctic fish species of the suborder Notothenioidei. *Biophys. J.* 93:2822–2829.
- Vitagliano, L., G. Bonomi, A. Riccio, G. di Prisco, G. Smulevich, et al. 2004. The oxidation process of Antarctic fish hemoglobins. *Eur. J. Biochem.* 271:1651–1659.
- Vitagliano, L., A. Vergara, G. Bonomi, A. Merlino, G. Smulevich, et al. 2008. Spectroscopic and crystallographic analysis of a tetrameric hemoglobin oxidation pathway reveals features of an intermediate R/T state. *J. Am. Chem. Soc.* 120:10527–10531.
- Johnston, I. A. 2003. Muscle metabolism and growth in Antarctic fishes (suborder Notothenioidei): evolution in a cold environment. *Comp. Biochem. Physiol. B.* 136:701–713.
- Verde, C., A. Vergara, D. Giordano, L. Mazzarella, and G. di Prisco. 2008. Hemoglobins of fishes living at polar latitudes: current knowledge on evolutionary and structural adaptation in a changing environment. *Curr. Protein Pept. Sci.* 9:578–590.
- Brittain, T. 2005. The Root effect in hemoglobins. *J. Inorg. Biochem.* 99:120–129.
- Verde, C., A. Vergara, E. Parisi, D. Giordano, L. Mazzarella, et al. 2007. The Root effect—a structural and evolutionary perspective. *Antarct. Sci.* 19:271–278.
- Perutz, M. F., and M. Brunori. 1982. Stereochemistry of cooperative effects in fish and amphibian hemoglobins. *Nature.* 299:421–426.
- Unzai, S., K. Imai, S.-Y. Park, K. Nagai, T. Brittain, et al. 2008. Mutagenic Studies on the Origins of the Root Effect. Springer, Milan, Italy.
- Mazzarella, L., G. Bonomi, M. C. Lubrano, A. Merlino, A. Vergara, et al. 2006. Minimal structural requirement of Root effect: crystal structure of the cathodic hemoglobin isolated from *Trematomus newnesi*. *Proteins.* 62:316–321.
- Mazzarella, L., A. Vergara, L. Vitagliano, A. Merlino, G. Bonomi, et al. 2006. High resolution crystal structure of deoxy hemoglobin from *Trematomus bernacchii* at different pH values: the role of histidine residues in modulating the strength of the Root effect. *Proteins.* 65:490–498.
- Yokoyama, T., K. T. Chong, G. Miyazaki, H. Morimoto, D. T. B. Shih, et al. 2004. Novel mechanisms of pH sensitivity in tuna hemoglobin: a structural explanation of the Root effect. *J. Biol. Chem.* 279:28632–28640.
- Giordano, D., A. Vergara, H. C. Lee, J. Peisach, M. Balestrieri, et al. 2007. Hemoglobin structure/function and globin-gene evolution in the Arctic fish *Liparis tunicatus*. *Gene.* 406:48–58.
- Camardella, L., C. Caruso, R. D'Avino, G. di Prisco, B. Rutigliano, et al. 1992. Hemoglobin of the Antarctic fish *Pagothenia bernacchii*. Amino acid sequence, oxygen equilibria and crystal structure of its carbonmonoxy derivative. *J. Mol. Biol.* 224:449–460.
- D'Avino, R., C. Caruso, M. Tamburrini, M. Romano, B. Rutigliano, et al. 1994. Molecular characterization of the functionally distinct hemoglobins of the Antarctic fish *Trematomus newnesi*. *J. Biol. Chem.* 269:9675–9681.
- Tamburrini, M., A. Brancaccio, R. Ippoliti, and G. di Prisco. 1992. The amino acid sequence and oxygen-binding properties of the single hemoglobin of the cold-adapted Antarctic teleost *Gymnodraco acuticeps*. *Arch. Biochem. Biophys.* 292:295–302.
- Giordano, D., L. Boechi, A. Vergara, M. A. Martí, U. Samuni, et al. 2008. The hemoglobins of the sub-Antarctic fish *Cottoperca gobio*,

- a phylogenetically basal species. Oxygen-binding equilibria, kinetics and molecular dynamics. *FEBS J.* 276:2266–2277.
28. Fukada, H., and K. Takahashi. 1998. Enthalpy and heat capacity changes for the proton dissociation of various buffer components in 0.1 M potassium chloride. *Proteins.* 33:159–166.
 29. Otwinowski, Z., and W. Minor. 1997. Processing of X-ray diffraction data collected in oscillation mode. *Methods Enzymol.* 276:307–326.
 30. Ito, N., N. H. Komiyama, and G. Fermi. 1995. Structure of deoxyhemoglobin of the Antarctic fish *Pagothenia bernacchii* with an analysis of the structural basis of the Root effect by comparison of the liganded and unliganded hemoglobin structures. *J. Mol. Biol.* 250:648–658.
 31. Sheldrick, G., and T. Schneider. 1997. SHELXL: high-resolution refinement. *Methods Enzymol.* 277:319–343.
 32. Jones, T. A., J. Y. Zou, S. W. Cowan, and M. Kjedaard. 1991. Improved methods for binding protein models in electron density maps and the location of errors in these models. *Acta Crystallogr. D Biol. Crystallogr.* 56:714–721.
 33. Everse, J., M. Johnson, and M. Marini. 1994. Peroxidative activities of hemoglobin and hemoglobin derivatives. *Methods Enzymol.* 231:547–559.
 34. Gabbianelli, R., G. Zolese, E. Bertoli, and G. Falcioni. 2004. Correlation between functional and structural changes of reduced and oxidized trout hemoglobins I and IV at different pHs. A circular dichroism study. *Eur. J. Biochem.* 271:1971–1979.
 35. Peisach, J. 1998. EPR of metalloproteins: truth tables revisited. In *Foundations of Modern EPR*. S. S. Eaton, G. R. Eaton, and K. Salikhov, editors. World Scientific Press, Singapore. 346–360.
 36. Ikeda-Saito, M., H. Hori, L. A. Andersson, R. C. Prince, I. J. Pickering, et al. 1992. Coordination structure of the ferric heme iron in engineered distal histidine myoglobin mutants. *J. Biol. Chem.* 267:22843–22852.
 37. Quillin, M., R. Arduini, J. Olson, and G. J. Phillips. 1993. High-resolution crystal structures of distal histidine mutants of sperm whale myoglobin. *J. Mol. Biol.* 234:140–155.
 38. Smulevich, G., A. Feis, and B. D. Howes. 2005. Fifteen years of Raman spectroscopy of engineered heme containing peroxidases: what have we learned? *Acc. Chem. Res.* 38:433–440.
 39. Ilari, A., A. Bonamore, A. Farina, K. Johnson, and A. Boffi. 2002. The X-ray structure of ferric *Escherichia coli* flavohemoglobin reveals an unexpected geometry of the distal heme pocket. *J. Biol. Chem.* 26:23725–23732.
 40. Marmo Moreira, L., A. Lima Poli, A. J. Costa-Filho, and H. Imasato. 2006. Pentacoordinate and hexacoordinate ferric hemes in acid medium: EPR, UV-Vis and CD studies of the giant extracellular hemoglobin of *Glossoscolex paulistus*. *Biophys. Chem.* 124:62–72.
 41. Boffi, A., S. Takahashi, C. Spagnuolo, D. L. Rousseau, and E. Chiancone. 1994. Structural characterization of oxidized dimeric *Scapharca inaequivalvis* hemoglobin by resonance Raman spectroscopy. *J. Biol. Chem.* 269:20437–20440.
 42. Smulevich, G. 1998. Understanding heme cavity structure of peroxidases: comparison of electronic absorption and resonance Raman spectra with crystallographic results. *Biospectroscopy.* 4:S3–S17.
 43. Hersleth, H. P., Y. W. Hsiao, U. Ryde, C. H. Görbitz, and K. K. Andersson. 2008. The influence of X-rays on the structural studies of peroxide-derived myoglobin intermediates. *Chem. Biodivers.* 5:2067–2089.
 44. Merlino, A., C. Verde, G. di Prisco, L. Mazzarella, and A. Vergara. 2008. Reduction of ferric hemoglobin from *Trematomus bernacchii* in a partial bis-histidyl state produces a deoxy coordination even when encapsulated into the crystal phase. *Spectroscopy.* 22:143–152.
 45. Baron, C. P., L. H. Skibsted, and H. J. Andersen. 2000. Peroxidation of linoleate at physiological pH: hemichrome formation by substrate binding protects against metmyoglobin activation by hydrogen peroxide. *Free Radic. Biol. Med.* 28:549–558.
 46. Baron, C. P., L. H. Skibsted, and H. J. Andersen. 2002. Concentration effects in myoglobin-catalyzed peroxidation of linoleate. *J. Agric. Food Chem.* 50:883–888.